⌘ *Author's Choice*

Dissecting the Metabolic Roles of Pteridine Reductase 1 in *Trypanosoma brucei* and *Leishmania major**

Han B. Ong, Natasha Sienkiewicz, Susan Wyllie, and Alan H. Fairlamb[1]
From the Division of Biological Chemistry & Drug Discovery, College of Life Sciences, University of Dundee, Wellcome Trust Biocentre, Dundee DD1 5EH, Scotland, United Kingdom

Leishmania parasites are pteridine auxotrophs that use an NADPH-dependent pteridine reductase 1 (PTR1) and NADH-dependent quinonoid dihydropteridine reductase (QDPR) to salvage and maintain intracellular pools of tetrahydrobiopterin (H_4B). However, the African trypanosome lacks a credible candidate *QDPR* in its genome despite maintaining apparent QDPR activity. Here we provide evidence that the NADH-dependent activity previously reported by others is an assay artifact. Using an HPLC-based enzyme assay, we demonstrate that there is an NADPH-dependent QDPR activity associated with both *Tb*PTR1 and *Lm*PTR1. The kinetic properties of recombinant PTR1s are reported at physiological pH and ionic strength and compared with *Lm*QDPR. Specificity constants (k_{cat}/K_m) for *Lm*PTR1 are similar with dihydrobiopterin (H_2B) and quinonoid dihydrobiopterin (qH_2B) as substrates and about 20-fold lower than *Lm*QDPR with qH_2B. In contrast, *Tb*PTR1 shows a 10-fold higher k_{cat}/K_m for H_2B over qH_2B. Analysis of *Trypanosoma brucei* isolated from infected rats revealed that H_4B (430 nM, 98% of total biopterin) was the predominant intracellular pterin, consistent with a dual role in the salvage and regeneration of H_4B. Gene knock-out experiments confirmed this: PTR1-nulls could only be obtained from lines overexpressing *Lm*QDPR with H_4B as a medium supplement. These cells grew normally with H_4B, which spontaneously oxidizes to qH_2B, but were unable to survive in the absence of pterin or with either biopterin or H_2B in the medium. These findings establish that PTR1 has an essential and dual role in pterin metabolism in African trypanosomes and underline its potential as a drug target.

Tetrahydrobiopterin (H_4B)[2] is a biologically significant pterin that functions as an essential cofactor for several enzymes. In mammalian cells these enzymes catalyze reactions such as the hydroxylation of aromatic amino acids (phenylalanine, tyrosine, and tryptophan) by their respective hydroxylases (1–3), as well as the hydroxylation and cleavage of glyceryl ethers by glyceryl-ether monooxygenase (4, 5). In addition, H_4B is also required for the coupling of all three isoforms of nitric-oxide synthases (NOS) for the production of nitric oxide (NO), both an important signaling molecule as well as a powerful antimicrobial agent (6–8). In mammalian cells, H_4B is synthesized *de novo* from guanosine triphosphate (GTP) and oxidized to H_4B-4a-carbinolamine following its utilization in hydroxylation reactions (9–11). The oxidized pterin is subsequently regenerated to its fully reduced form via the quinonoid dihydrobiopterin (qH_2B) intermediate by the enzymes pterin 4a-carbinolamine dehydratase (PCD; EC 4.2.1.96) and quinonoid dihydropteridine reductase (QDPR; 6,7-dihydropteridine reductase, EC 1.5.1.34) (12–14). qH_2B can also be non-enzymatically generated by the spontaneous oxidation of H_4B before undergoing further rearrangement to form 7,8-dihydrobiopterin (H_2B), a process accelerated by the presence pro-oxidants (15–17). H_2B can then be reduced to H_4B by mammalian dihydrofolate reductase (DHFR), a key enzyme in folate metabolism, in an alternative salvage reaction (18).

Protozoan parasites in the family Trypanosomatidae are the causative agents of several neglected tropical diseases, including the leishmaniases, caused by the *Leishmania spp.* and the African trypanosomiases caused by *Trypanosoma brucei ssp*. The current understanding of pterin metabolism in trypanosomatids stems largely from studies on *Leishmania spp.* and also the insect trypanosomatid, *Crithidia fasciculata*. These parasites lack the biosynthetic pathway to H_4B and are auxotrophic for pterins (19–21). In *Leishmania*, salvage of extracellular biopterin involves uptake predominantly through the biopterin transporter 1 (BT1) and the fully oxidized pterin is then reduced sequentially to its dihydro- and tetrahydro-forms by the NADPH-dependent enzyme pteridine reductase 1 (PTR1; EC 1.5.1.33) (22, 23). The end product of this salvage pathway (H_4B) is essential for growth of the promastigote stage of *Leishmania major*, because PTR1-null mutants are unable to grow in culture unless supplemented with H_2B or H_4B (23).

The precise functions of H_4B within *Leishmania spp.* are not fully understood. H_4B deficiency in the insect vector (promastigote) stage of the life cycle promotes increased differentiation into the mammalian-infectious metacyclic promastigote form (24), but the underlying mechanism remains obscure. Unlike mammalian cells, glyceryl-ether monooxygenase in *Leishmania donovani* is dependent upon NADPH instead of H_4B (25). With the exception of phenylalanine hydroxylase (PAH), genes for NOS and other aromatic amino acid hydroxylases are not annotated in any *Leishmania* genome. Moreover, *Lm*PAH appear to be non-essential for the growth of *L. major in vitro* (26) indicating that there must be other crucial pterin-depen-

---

[2] The abbreviations used are: H_4B, 5,6,7,8-tetrahydrobiopterin; H_2B, 7,8-dihydrobiopterin; qH_2B, quinonoid 7,8-dihydrobiopterin; DMH_4P, 6,7-dimethyl-5,6,7,8-tetrahydrodropterin; $qDMH_2P$, quinonoid 6,7-dimethyl-7,8-dihydropterin; PTR1, pteridine reductase 1; QDPR, quinonoid dihydropteridine reductase.

dent processes within these parasites. Whatever the role(s) of H$_4$B within these parasites may be, *L. major* also harbor a putative PCD and a well-characterized QDPR (27) suggesting they are able to regenerate H$_4$B in a fashion not unlike mammalian cells. A role for H$_4$B in defense against oxidative stress in *Leishmania* has also been suggested by two independent studies, where PTR1-null mutants of *L. major* showed increased susceptibility to oxidative stress (28, 29). However, the underlying mechanism remains unclear.

In contrast to the leishmania parasites, very little is known about pterin metabolism in *T. brucei*. However, it would appear to be considerably different. Knockdown of PTR1 levels in *T. brucei* by RNA interference is lethal *in vitro* and cannot be rescued by supplementation with either H$_2$B or H$_4$B (30), unlike *L. major* PTR1-null mutants (24). In addition, PTR1 knockdown abolishes infectivity of *T. brucei* to mice (30), unlike *L. major ptr1$^{-/-}$* that retains infectivity to mice (24). Finally, despite a report of QDPR activity in *T. brucei* (27), no obvious candidate genes for QDPR (or PAH) have been identified in its genome. The current study provides an explanation for some of these anomalies and provides convincing evidence that PTR1 is an essential drug target in the African trypanosome, *T. brucei*.

EXPERIMENTAL PROCEDURES

Organisms and Reagents—All pterins were purchased from Schircks laboratories. Other chemicals and reagents used in this study were of the highest grade and purity available. *T. brucei* procyclic-form strain 29–13 (31) was cultured at 28 °C in SDM-79 medium (32) supplemented with 50 μg ml^{-1} hygromycin (Roche) and 15 μg ml^{-1} gentamycin sulfate (G418, Invitrogen). *T. brucei* bloodstream-form "single marker" S427 was cultured at 37 °C in either HMI-9T medium (33) or low folate medium (34), with both media supplemented with 15 μg ml^{-1} of G418. Alternatively, parasites were purified from infected rat blood (35). Additional H$_4$B (1 μM) was included in cultures of *T. brucei* cells expressing *Lm*QDPR.

Analysis of Pterins by HPLC—Reverse-phase HPLC was carried out on an ion-paired Ultrasphere C$_{18}$ column (HPLC Technology) using a Dionex UltiMate 3000 system coupled to a Dionex RF-2000 fluorometer. Pterins were separated and eluted using an isocratic mobile phase of 20 mM (Na$^+$) phosphate pH 6.5, 4% (v/v) methanol at a flow rate of 1 ml min^{-1}. Prior to HPLC analysis, biological samples were oxidized with iodine in the presence of 0.1 M HCl or NaOH (36, 37). Precipitated proteins were removed by centrifugation (20,000 $\times$ *g*, 4 °C, 20 min) and supernatants analyzed by HPLC. Oxidized pterins were detected fluorometrically using excitation and emission wavelengths of 360 and 440 nm, respectively. Biopterin plus H$_2$B was quantified by determining the total biopterin in alkaline-oxidized samples. Concentrations of H$_4$B were calculated by subtracting total biopterin in alkaline-oxidized samples from total biopterin in acid-oxidized samples. Pterin standards were quantified using published extinction coefficients (38).

Pterin Content in T. brucei and Mouse Serum—Parasites were harvested by centrifugation (800 $\times$ *g*, 4 °C, 10 min) and washed once with phosphate buffered saline (PBS, Invitrogen).

Cell pellets were resuspended in PBS and aliquots (100 μl) were oxidized, deproteinized, and analyzed as above.

The concentration of pterins in serum from infected and uninfected mice were determined by infecting 25 Balb/c mice with 1 $\times$ 10^5 bloodstream *T. brucei* parasites via intra-peritoneal injection. Parasitaemia was evaluated as previously described (34). Groups of 5 mice were exsanguinated under anesthesia on day zero and daily thereafter until a lethal parasitaemia was achieved on day 4. Blood samples were allowed to clot, centrifuged (1,000 $\times$ *g*, 4 °C, 10 min) and aliquots of supernatant (100 μl) were immediately oxidized, deproteinized, and analyzed by HPLC.

Enzyme Kinetics—*Lm*PTR1 from *Lm*PTR1_pET3a (23) was cloned into the pET15b vector. Histidine-tagged recombinant *Tb*PTR1, *Lm*PTR1, and *Lm*QDPR were expressed and purified as published (27, 39, 40). *Lm*PTR1 and *Lm*QDPR were further purified to homogeneity by anion-exchange chromatography (39). *PTR1 activity* was measured by HPLC using H$_2$B as a substrate (37) and spectrophotometrically on a UV-1601 spectrophotometer (Shimadzu) using the quinonoid substrates qH$_2$B or qDMH$_2$P generated from the corresponding tetrahydropterins using horseradish peroxidase (HRP) and H$_2$O$_2$ (27). Rates of oxidation of NADPH or NADH at 340 nm were calculated using the extinction coefficient 6.22 mM cm^{-1}. Initial linear rates were measured over 120 s and corrected for nonspecific oxidation of NADH or NADPH. One unit of enzyme activity is defined as one μmol of substrate used (spectrophotometric assays) or product formed (HPLC) per min.

The pH optimum of *Tb*PTR1 for H$_2$B was determined using overlapping buffers of sodium citrate (pH 2.6 to 5.5) and HEPES/MES/CHES (pH 5.5–10), adjusted to a constant ionic strength of 150 mM with NaCl. All subsequent enzymatic assays were carried out in 50 mM HEPES buffer, adjusted to pH 7.4 and an ionic strength of 100 mM using KOH and KCl. All assay mixtures were pre-equilibrated to 25 °C before the reaction was initiated by the addition of the appropriate pterin substrate.

The K_m^{app} of *Tb*PTR1 for NADPH was determined using a fixed concentration of the enzyme (1.1 nM) and H$_2$B (25 nM) in the presence of varying concentrations of NADPH (0.2–200 μM). Using 1.1 nM enzyme and 100 μM NADPH cofactor, the concentration of H$_2$B was varied from 10 to 3000 nM to determine the K_m^{app} of *Tb*PTR1 for H$_2$B. For *Lm*PTR1, the concentration of enzyme was increased to 5 nM and H$_2$B concentration varied from 50 to 4000 nM. The K_m^{app} of *Tb*PTR1 and *Lm*PTR1 with the quinonoid dihydropterin substrates were determined in the same buffer by varying the concentrations of tetrahydropterins from 0.8 to 100 μM in the presence of 85 nM enzyme, 50 μM NADPH, 20 μg ml^{-1} HRP, and 0.9 mM H$_2$O$_2$. These results were fitted by non-linear regression to Equation 1 for high substrate inhibition in GraFit.

$$\nu = \frac{V_{max}}{1 + \frac{K_m}{S} + \frac{S}{K_i^s}} \qquad \text{(Eq. 1)}$$

The K_m^{app} of *Lm*QDPR for the quinonoid substrates were measured in a similar fashion, using 2 nM enzyme and 50 μM NADH. Data were fitted to the Michaelis-Menten equation.

Knock-out of PTR1 in Bloodstream Form T. brucei—Knock-out constructs of *Tb*PTR1 were prepared as previously described (30). To generate the tetracycline-inducible *LmQD-PR*_pLew82 overexpression construct, the open reading frame of the gene was amplified from the *LmQDPR*_pET15b construct using primers 5′-gcgc**aagcttc**atgaaaaatgtactcctcatcg-3′ and 5′-gcgc**ggatcc**ctacacaataaaacgcgtcttcg-3′ (restriction enzymes sites HindIII and BamHI highlighted in bold italics, respectively) and cloned into the pLew82 vector (31). *LmQD-PR*_pLew82 was transfected into wild-type (WT) bloodstream form *T. brucei* by electroporation for targeted integration into the ribosomal DNA locus (31) and parasites overexpressing *Lm*QDPR (^{oe}WT) selected for resistance to phleomycin (5.0 μg ml^{-1}, InvivoGen). A cloned cell line of ^{oe}WT was generated by limiting dilution and used for subsequent studies. Single (^{oe}SKO) and double knock-out lines (^{oe}DKO) of *Tb*PTR1 were generated using puromycin and hygromycin selection (30).

Southern Analysis—Genomic DNA (5 μg) was prepared and digested with SacI and SphI for Southern analysis (30). Probes of the open reading frames of *TbPTR1* and *LmQDPR* were prepared using the PCR DIG Probe Synthesis Kit (Roche). The blot was sequentially probed and processed using the DIG Detection kit (Roche), according to the manufacturer's instructions.

Semi-quantitative RT-PCR—Levels of *TbPTR1* and *LmQDPR* mRNA in WT and transfected parasites were determined by semi-quantitative RT-PCR analysis using the One Step RT-PCR Kit (Qiagen), according to the manufacturer's instructions. RNA was prepared from log-phase (1×10^6 cells ml^{-1}) cultures of bloodstream trypanosomes using RNeasy mini prep kit (Qiagen). DNA was removed from samples using the DNAfree kit (Ambion) and RNA was quantified at 260/280 nm using a Biowave II spectrophotometer (VWP). Oligonucleotide sequences of *TbPTR1* (5′-TGT-ACGTCGTCGAATCTT-3′ and 5′-AACCAATGCGTGTTT-ACC-3′) and *LmQDPR* (5′-GCTGAGACAATCGCTCTT-3′ and 5′-TGAGAAGAAGCAGTCCATT-3′) were designed using the Beacon Design software (PREMIER Biosoft International) to generate products of 102 and 83 bp, respectively. RNA (0.5 μg) from each cell type was reverse transcribed using the following conditions: 50 °C × 30 min and 95 °C × 15 min for 1 cycle; followed by 95 °C × 1 min, 60 °C × 1 min and 72 °C × 1 min for 30 cycles; and a final extension at 72 °C × 10 min for 1 cycle. PCR products were analyzed by agarose gel-electrophoresis.

Preparation of Cell Lysates for Enzymatic Studies—Log-phase cultures of *T. brucei* (1×10^7 cells ml^{-1} for procyclics; 1×10^6 cells ml^{-1} for bloodstream) were harvested by centrifugation ($800 \times g$, 10 min, 4 °C) and washed twice with PBS. Clarified lysates of parasites were prepared as published (33). Trypanothione reductase activity in lysates was determined to ensure adequate extraction of parasites (41). Specific activities of PTR1 and *q*DPR were determined using 25 nM H$_2$B plus 100 μM NADPH or 4 μM H$_4$B or 10 μM DMH$_4$P plus 100 μM NADH as substrates, respectively.

RESULTS

Intracellular Pterin Analysis of T. brucei—Initial studies established that pterin standards can be optimally separated and quantified on a C$_{18}$ column using an isocratic mobile phase containing 20 mM (Na$^+$) phosphate and 4% methanol (Fig. 1*A*).
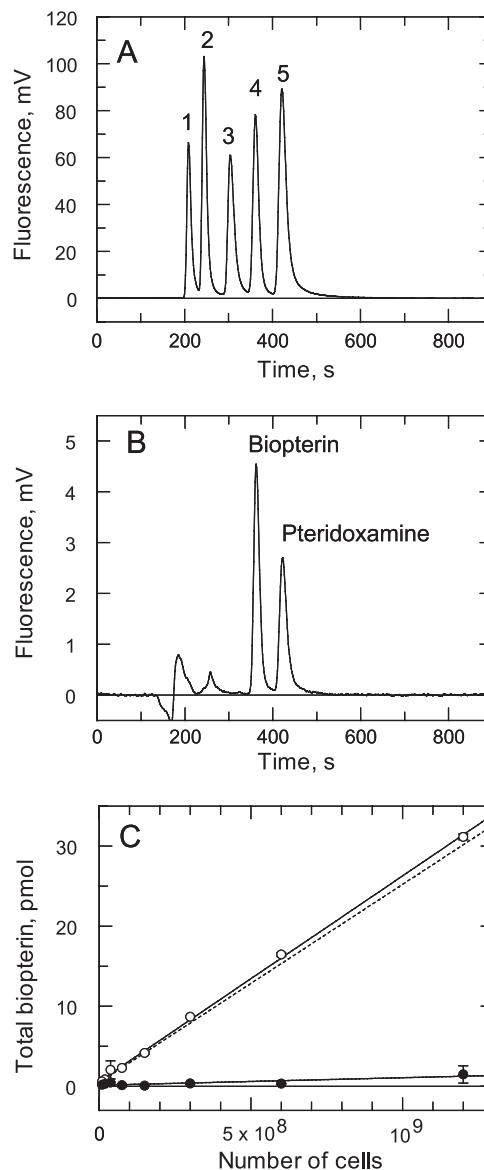

FIGURE 1. **Intracellular pterin analysis of *T. brucei*.** *A*, chromatogram of pterin standards. *Peak 1*, pterin-6-carboxylate (2.5 pmol); *peak 2*, neopterin (5 pmol); *peak 3*, xanthopterin (10 pmol); *peak 4*, biopterin (5 pmol); and *peak 5*, pteridoxamine (10 pmol). *B*, chromatogram of extracts of bloodstream trypanosomes recovered from rats following oxidation with iodine under acidic conditions. *C*, biopterin content as a function of cell number. Total biopterin (○); biopterin plus H$_2$B (●). The *dashed line* represents the net H$_4$B content. Bloodstream trypanosomes were oxidized with iodine under acidic conditions and analyzed by HPLC as described under "Experimental Procedures." Each data point is the mean ± S.E. ($n = 3$).

Biopterin is the major intracellular pterin in bloodstream form *T. brucei* harvested from infected rats (Fig. 1*B*). Total biopterin content is proportional to cell number between 1×10^7 and 1.2×10^9 per assay (Fig. 1*C*), yielding a total biopterin content of 2.57 ± 0.03 pmol per 10^8 cells. This is equivalent to 440 nM, based on a cell volume of 5.8 μl (42). Differential oxidation under acidic or alkaline conditions indicated that H$_4$B plus *q*H$_2$B constituted more than 96% (430 nM) of the total intracellular biopterin. The fluorescent peak which co-elutes with pteridoxamine (2-amino-1H-pteridin-4-one or "pterin") (Fig. 1*B*), is likely to be derived from tetrahydrofolate, following oxidation by iodine under acidic conditions (36).

Pterin Content of Serum from T. brucei-infected Mice—In previous studies, elevated levels of NOS activity and NO have been observed in *T. brucei*-infected animals (43). H_4B is required for the production for NO and circulating levels of H_4B can be elevated as a mechanism of immune system activation (44, 45). To examine if infection with *T. brucei* stimulates H_4B production *in vivo*, biopterin concentrations were determined during the course of the infection (Fig. 2). In keeping with previous studies (36, 38), the basal level of total biopterin in uninfected mouse serum was determined to be 128 ± 19 nM of

which 57% was recovered as H_4B. As the infection progressed total biopterin in serum gradually increased reaching 292 ± 8 ($n = 5$) nM by day 4 when parasitaemia was at its peak ($\sim 1 \times 10^9$ ml^{-1}). The levels of biopterin plus H_2B remained relatively constant throughout the study, whereas H_4B increased ~ 3-fold from 73 ± 14 nM on day 0 to 230 ± 6 on day 4. Thus, infection with *T. brucei* does indeed stimulate H_4B production in the host.

Kinetic Studies on TbPTR1—PTR1 is pivotal for salvage of biopterin in trypanosomatids, with its essentiality in *T. brucei* previously established by RNA interference studies (30). Kinetic parameters of *Tb*PTR1 for the reduction of H_2B vary considerably (37, 39), depending upon the pH optimum (3.7 *versus* 6.0), enzyme concentration (4.8 *versus* 700 nM) and the assay format (direct spectrophotometric *versus* cytochrome *c*-coupled method). Because PTR1 has been determined to be a cytosolic enzyme in *T. brucei* (30), the pH optimum of the enzyme was re-examined using H_2B as substrate. Using the HPLC-based assay, the enzyme displays a bell shaped pH profile with a broad pH optimum from 5.5 to 8 for H_2B (Fig. 3*A*). Because the reported cytosolic pH of *T. brucei* is 7.4 (46), recombinant *Tb*PTR1 was subsequently characterized at this physiologically relevant pH and ionic strength.

As previously observed under different assay conditions (37, 39), H_2B was found to inhibit *Tb*PTR1 at high substrate concentrations, yielding a $K_m^{app} = 29.4$ nM, $K_i^s = 1.2$ μM, and $k_{cat}/K_m = 1.7 \times 10^6$ M^{-1} s^{-1} (Fig. 3*B*; Table 1). The K_m
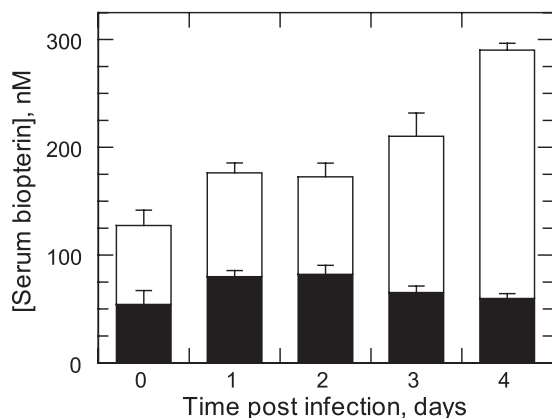

FIGURE 2. **Pterin content of mouse serum during the course of infection with *T. brucei*.** Blood samples were analyzed by HPLC as described under "Experimental Procedures." Biopterin plus H_2B (*black bars*) or H_4B (*white bars*). Each data point is the mean $\pm$ S.E. ($n = 5$), except for day 0 ($n = 4$).
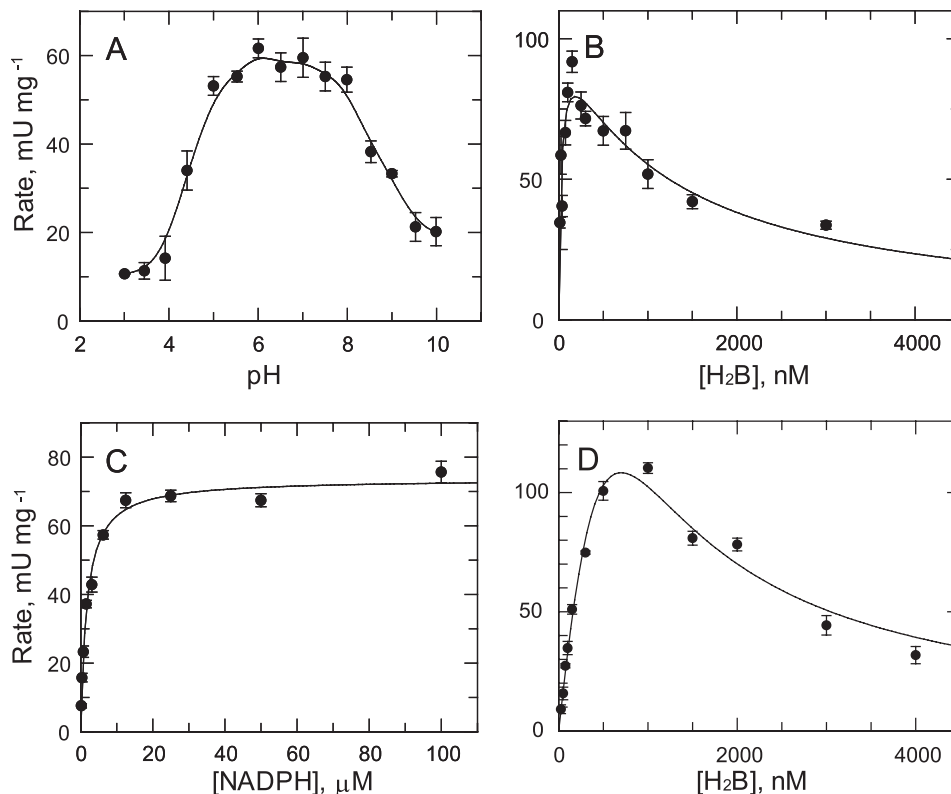

FIGURE 3. **Kinetic characterization of *Tb*PTR1 using H_2B as substrate.** *A*, pH optimum of *Tb*PTR1 for H_2B determined using a constant ionic strength overlapping buffer system. *B*, rate behavior of *Tb*PTR1 as a function of H_2B concentration. *C*, rate behavior of *Tb*PTR1 as a function of NADPH concentration. *D*, rate behavior of *Lm*PTR1 for H_2B in comparison to *Tb*PTR1. PTR1 activity was measured using an HPLC-based assay as described under "Experimental Procedures." Each data point is the mean $\pm$ S.E. ($n = 3$). The *solid lines* represent the unweighted non-linear fit to either the substrate inhibition equation or Michaelis-Menten equation. Kinetic parameters are reported in Table 1.

TABLE 1

Summary and comparison of the kinetic characterization of *Tb*PTR1, *Lm*PTR1, and *Lm*QDPR with various substrates

		*Tb*PTR1			*Lm*PTR1			*Lm*QDPR	
	Units	H$_2$B	qH$_2$B	qDMH$_2$P	H$_2$B	qH$_2$B	qDMH$_2$P	qH$_2$B	qDMH$_2$P
K_m^{app}	μM	0.0294 ± 0.0061	3.36 ± 0.70	16.6 ± 1.9	3.32 ± 0.48	10.3 ± 1.5	21.0 ± 4.3	4.12 ± 0.44	22.8 ± 3.0
K_i^s	μM	1.16 ± 0.27	3.14 ± 0.70	475 ± 91	0.15 ± 0.022	1.22 ± 0.29	92.2 ± 18.9	NA[a]	NA
k_{cat}	s^{-1}	0.05	0.54	0.43	0.57	1.84	0.44	16.2	22.7
k_{cat}/K_m^{app}	M^{-1} s^{-1}	17×10^5	1.6×10^5	0.26×10^5	1.7 × 10^5	1.8×10^5	0.21×10^5	39×10^5	10×10^5

[a] Not applicable.

TABLE 2

PTR1 and QDPR activities in *T. brucei* lysates

Trypanothione reductase (TryR) activities were determined as a positive control to ensure adequate extraction of parasites and were found to be in good agreement with the previously published values (51).

Enzyme/lysate	PTR1[a]	QDPR[b]	TryR
	mU mg^{-1}	mU mg^{-1}	mU mg^{-1}
Bloodstream-form *T. brucei* from rats	0.029 ± 0.001	<1	63.3 ± 1.7
Bloodstream-form *T. brucei* from culture	0.031 ± 0.001	<1	72.6 ± 2.6
Procyclic-form *T. brucei* from culture	0.029 ± 0.002	<1	109.2 ± 1.5
Bloodstream-form *T. brucei* overexpressing *Lm*QDPR (ᵒᵉWT)	0.025 ± 0.003	64.3 ± 5.7	75.9 ± 2.8

[a] Determined by HPLC method with 25 nM H$_2$B and 100 μM NADPH.
[b] Determined by spectrophotometric method with 4 μM qH$_2$B and 100 μM NADH.

determined at pH 7.4 was within experimental error to that previously reported at pH 6.0 (25 ± 6.7 nM) using the HPLC-based method, but was 30-fold less susceptible to substrate inhibition (1.2 μM *versus* 37 nM for pH 7.4 and 6.0, respectively). When assayed under identical conditions, the equivalent kinetic parameters for *Lm*PTR1 with H$_2$B as varied substrate, the resulting K_m^{app}, K_i^s, and k_{cat}/K_m values were 3.3 μM, 0.15 μM, and 1.7 × 10^5 M^{-1} s^{-1}, respectively (Fig. 3D; Table 1). The K_m^{app} value is within experimental error of the previously reported value (5.4 ± 2.3 μM), determined spectrophotometrically in phosphate buffer at pH 7.0 (20). However, K_i^s is markedly different (0.15 *versus* 18.2 ± 2.7 μM). The reason for this discrepancy is not clear, but could be due to differences in the assay method, the pH and ionic strength of the buffer or the use of His-tagged enzyme in the current study.

Under the physiological assay conditions used here, *Tb*PTR1 was found to obey simple Michaelis-Menten kinetics when NADPH concentration was varied in presence of a fixed concentration of H$_2$B (25 nM), yielding a K_m^{app} of 1.7 ± 0.1 μM (Fig. 3C). The spectrophotometric method is too insensitive to measure PTR1 activity in cell lysates, but, using the more sensitive HPLC-based method, bloodstream-form and procyclic-form *T. brucei* have identical levels of enzyme activity (Table 2). Based on the specific activity of recombinant *Tb*PTR1 measured under identical conditions (73.6 ± 1.3 mU mg^{-1}), PTR1 constitutes ~0.04% of the total soluble protein in whole cells, equivalent to an enzyme concentration of ~2.5 nM or 87 molecules per cell.

PTR1 Can Reduce Quinonoid Dihydropterins—We have noted previously that reduction of cytochrome *c* by H$_4$B in our coupled assay for PTR1 was 40-fold greater than the theoretical yield for a single round of reduction of H$_2$B to H$_4$B (37). Because H$_4$B is oxidized in a sequential one electron reduction by cytochrome *c* to produce qH$_2$B (47), we investigated whether qH$_2$B could be an alternative substrate for *Tb*PTR1.

Initial studies indicated that *Tb*PTR1 could indeed reduce quinonoid dihydropterins in a reaction that is specific for

NADPH, unlike QDPR which has a strong preference for NADH (27). As observed with H$_2$B, qH$_2$B also inhibited *Tb*PTR1 at high substrate concentrations (Fig. 4A; Table 1). Substrate inhibition was evident, but less pronounced when the quinonoid form of the H$_4$B analog 6,7-dimethyltetrahydropterin (DMH$_4$P) was used as substrate (Fig. 4D; Table 1). Based on the specificity constants (k_{cat}/K_m) in Table 1 *Tb*PTR1 has a substrate preference in the order H$_2$B > qH$_2$B > qDMH$_2$P.

Unexpectedly, recombinant PTR1 from *L. major* was also found to be able to reduce both of these quinonoid substrates, with similar specificity for the cofactor NADPH and susceptibility to substrate inhibition. These findings are at odds with previous reports that *Lm*PTR1 is unable to catalyze these reactions (27, 48). The kinetic parameters (K_m, K_i^s, and k_{cat}) for *Lm*PTR1 were found to be within 3-fold of the values observed for *Tb*PTR1, although *Lm*PTR1 was more susceptible to substrate inhibition by qDMH$_2$P (Fig. 4, B and E; Table 1).

The efficiency of both PTR1 enzymes in reducing quinonoid dihydropterins was directly compared with the authentic and well-characterized QDPR from *L. major* (27). The kinetic parameters of *Lm*QDPR with qDMH$_2$P as substrate were found to be consistent with previously published values (27). Comparing the two substrates, *Lm*QDPR exhibited a lower K_m^{app} (~5-fold) as well as a higher catalytic efficiency (~4-fold) with its natural substrate, qH$_2$B, than with qDMH$_2$P (Fig. 4, E and F; Table 1). Interestingly, these K_m^{app} values were also found to be very similar to those determined for trypanosomatid PTR1 enzymes. However, inhibition by high qH$_2$B concentrations was not observed with *Lm*QDPR. Collectively, these results suggest that these enzymes have a higher affinity and a substrate preference for qH$_2$B over qDMH$_2$P. More significantly, the lower k_{cat}/K_m values also suggested that both PTR1 enzymes are less catalytically efficient in reducing quinonoid dihydropterins compared with *Lm*QDPR.

QDPR Activity in T. brucei Extracts—The ability of recombinant *Tb*PTR1 to reduce quinonoid substrates suggested that this enzyme could be responsible for the QDPR activity previously detected in lysates of procyclic-form *T. brucei* (27).
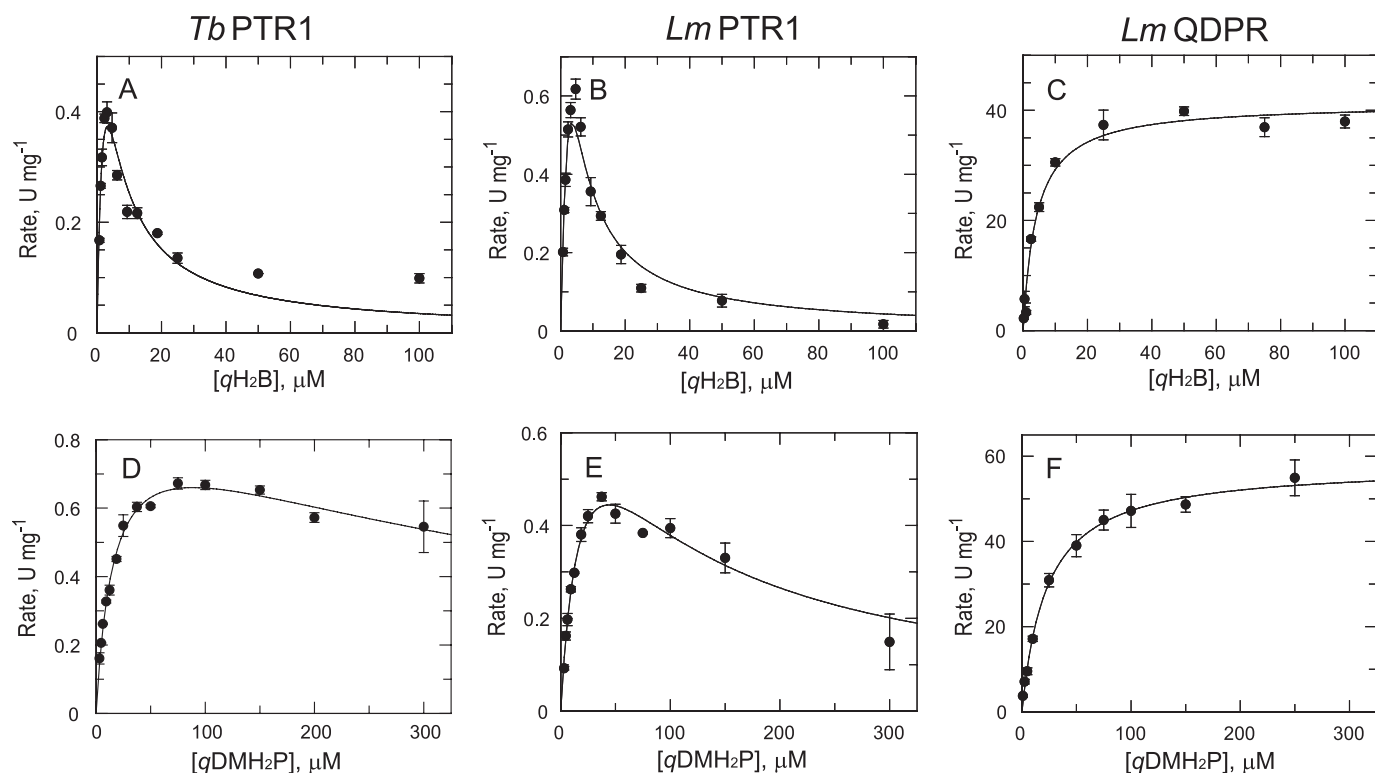
FIGURE 4. **Comparative studies of the reduction of quinonoid dihydropterins by *Tb*PTR1, *Lm*PTR1, and *Lm*QDPR.** PTR1 activity was determined by HPLC and QDPR activity was measured spectrophotometrically as described under "Experimental Procedures." *A* and *D*, rate behavior of *Tb*PTR1 as a function of varying substrate concentrations for qH_2B and $qDMH_2P$, respectively, determined in the presence of a fixed (saturating) concentration of NADPH. *B* and *E*, rate behavior of *Lm*PTR1 as a function of varying concentrations of qH_2B and $qDMH_2P$, respectively, determined in a similar fashion. *C* and *F*, rate behavior of *Lm*QDPR as a function of varying substrate concentrations of qH_2B and $qDMH_2P$, respectively, determined in the presence of a fixed (saturating) concentration of NADH. Each data point is the mean $\pm$ S.E. ($n = 3$). The *solid lines* represent the unweighted non-linear fit to either the substrate inhibition equation (PTR1) or Michaelis-Menten equation (QDPR). Kinetic parameters are reported in Table 1.

However, the QDPR activity in these lysates was apparently NADH-dependent, while, as shown here, *Tb*PTR1 is specific for NADPH as cofactor in its reduction of quinonoid dihydropterins.

Using NADH and $qDMH_2P$ (generated from DMH_4P by HRP and H_2O_2) we were able to confirm the presence of QDPR activity in extracts of *L. major* promastigotes with a specific activity of 33.1 ± 1.5 mU mg^{-1}, in good agreement with published data (27). An apparent QDPR activity was also present with $qDMH_2P$ in procyclic-form of *T. brucei* as illustrated by the spectrophotometric traces shown in Fig. 5*A*. After establishing the baseline rate of oxidation of NADH for 5 min, DMH_4P was added to the reaction mixtures to initiate the reaction. With *T. brucei* extract (*solid blue line*) there was an initial rapid decrease in absorbance that returned to the background rate of NADH oxidation as illustrated by the two *dotted blue lines*. The magnitude of this displacement was proportional to the amount of extract added to the assay (not shown) and the reaction was completely abolished by heat treatment of the enzyme sample (Fig. 5*A*, *gray line*). No such activity was observed with (mammalian) bloodstream form extracts (Fig. 5*A*, *green line*). Addition of *Lm*QDPR to the procyclic extract led to a complete oxidation of NADH (Fig. 5*A*, *purple line*), as would be expected based on the recycling nature of the assay. In contrast to the non-linear behavior of the procyclic extract (Fig. 5*B*, *blue line*), oxidation by the *L. major* enzyme extract was completely linear for the initial 200 s (Fig. 5*B*, *red line*) and did

not return to baseline levels during the experiment. Moreover, this phenomenon with extracts of *T. brucei* (insect) procyclic forms appears to be specific to $qDMH_2P$ as substrate, because it was not observed when qH_2B was used as substrate (Fig. 5*B*, *blue line*) and the residual rate was zero after correction for the non-enzymatic oxidation of NADH (Fig. 5*B*, *black line*). In contrast, *L. major* extract showed substantial NADH-dependent activity with qH_2B (Fig. 5*B*, *red line*) as did recombinant *Lm*QDPR (*purple line*). These findings demonstrate that DMH_4P is not a suitable substrate for determining QDPR activity in procyclic-form *T. brucei*.

Although QDPR activity with qH_2B and NADH was observed with *L. major* extracts, activity could not be detected in lysates of wild-type *T. brucei* in the presence of NADH, whereas it was readily measurable in *T. brucei* cell lines overexpressing *Lm*QDPR (Table 2). No PTR1-dependent QDPR-like activity could be detected with qH_2B and NADPH in *T. brucei* lysates using the spectrophotometric method. However, even though the specific activity of recombinant *Tb*PTR1 for qH_2B is 5-fold higher than H_2B (360 *versus* 73.6 mU mg^{-1}, respectively) the activity with qH_2B as substrate would still be too low for detection by this method. Unfortunately, our current HPLC method is unable to distinguish between the substrate, qH_2B and the product of the reaction, H_4B.

Knock-out of PTR1 in Bloodstream Form T. brucei—PTR1-null mutants of *L. major* have been previously shown to be viable provided the culture medium was supplemented with either
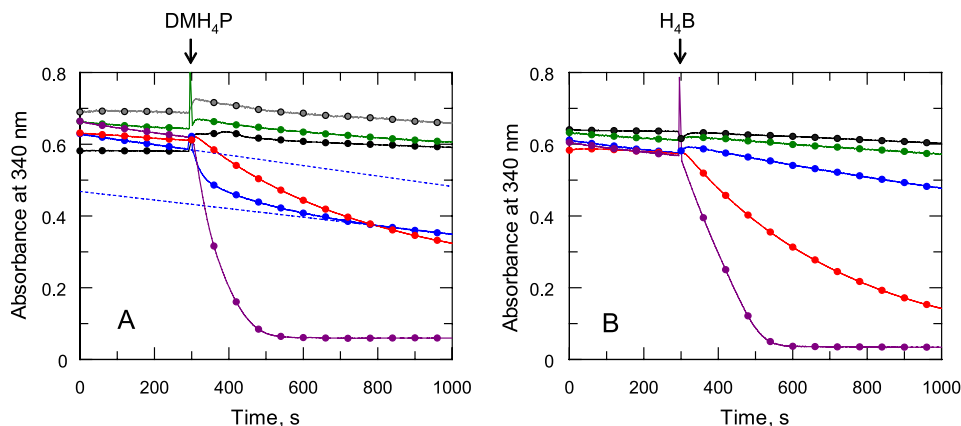
FIGURE 5. **Spectrophotometric traces for QDPR activity in lysates of *T. brucei* (bloodstream and procyclics) and *L. major* promastigotes.** Lysates were preincubated with HRP, H_2O_2, and NADH for 300 s before reactions were initiated by the addition of the tetrahydropterins indicated by the *arrows*. *A*, oxidation of NADH in assays carried out using $qDMH_2P$ as substrate. *Black line*, no extract; *blue*, plus 200 μg ml^{-1} procyclic-form *T. brucei* lysate; *purple*, procyclic-form *T. brucei* spiked with 1 μg of recombinant *Lm*QDPR; *gray*, heat-inactivated procyclic-form *T. brucei*; *green* 200 μg ml^{-1} bloodstream-form *T. brucei* lysate; and *red*, 200 μg ml^{-1} *L. major* promastigote lysate. *B*, assays using qH_2B as substrate. Reaction traces are as in *A*.
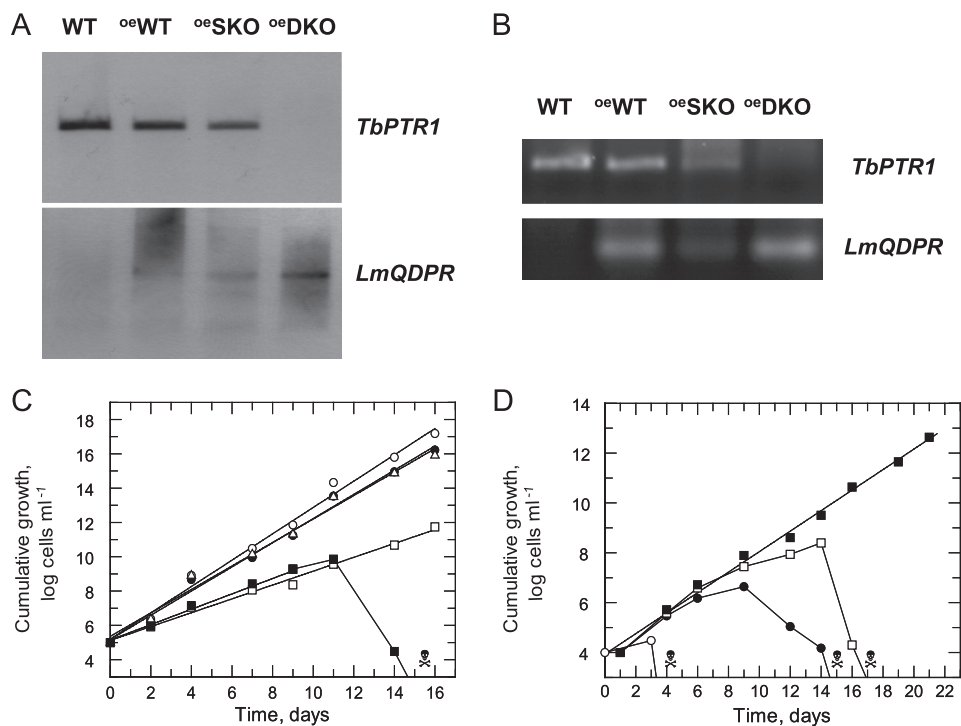

FIGURE 6. **Knock-out of TbPTR1 in bloodstream-form *T. brucei*.** *A*, Southern blot analysis of the genomic DNA from WT, [oe]WT, [oe]SKO, and [oe]DKO parasites. DNA was digested with SacI/SphI and probed sequentially with *TbPTR1* (*top panel*) and *LmQDPR* (*bottom panel*). *B*, confirmation of the loss of PTR1 transcript and the presence of QDPR in the [oe]DKO by RT-PCR. RNA samples were prepared as described under "Experimental Procedures." *C*, cumulative growth in HMI-9T medium plus H_4B of WT (○), [oe]WT (●), [oe]SKO (△), and [oe]DKO1(□) lines. This experiment is representative of five separate clones. Freshly prepared 1 μM H_4B was added at every subculturing step. [oe]DKO was cultured in the absence of H_4B (■). *D*, effect of various pterins on growth in low folate medium of [oe]WT cells. [oe]DKO, no pterin supplement (○); [oe]DKO, plus biopterin (●); [oe]DKO, plus H_2B (□); and [oe]DKO, plus H_4B (■) parasites. This experiment is representative of two separate clones. Freshly prepared 1 μM pterin was added at every subculturing step. Cell densities are the mean of duplicate measurements, and error bars are smaller than symbols.

H_2B or H_4B (23). When similar attempts to knock-out PTR1 in *T. brucei* were carried out in growth medium supplemented with H_2B or H_4B (or a combination of both), PTR1-null mutants could not be obtained (30). Bearing in mind the instability of H_4B in neutral or alkaline solutions, it is likely that H_4B was rapidly oxidized to qH_2B in culture medium (15–17). Because PTR1 is likely to be solely responsible for the regeneration of H_4B in *T. brucei*, we investigated whether a functional QDPR plus supplementation with H_4B could serve as an effective metabolic rescue strategy.

First, bloodstream *T. brucei* was transfected with the tetracycline-inducible *LmQDPR*_pLew82 vector construct and trypanosomes selected for stable integration into the ribosomal DNA locus by selection for resistance to phleomycin. The successful generation of a wild-type QDPR overexpressing cell line ([oe]WT) was verified by Southern blot analysis (Fig. 6*A*), and by RT-PCR (Fig. 6*B*). Because of the "leaky" nature of the promoter of pLew82, tetracycline induction was not required for cells to express measurable levels of *Lm*QDPR mRNA (Fig. 6*B*). In contrast to WT *T. brucei*, it was now possible to measure QDPR

activity in the extracts of [oe]WT parasites demonstrating that *Lm*QDPR is functionally active (Table 2). Parasites expressing *Lm*QDPR (doubling time, 8.4 h) were also found to have marginally slower growth rates than WT trypanosomes (doubling time, 6.9 h), suggesting that the QDPR might be toxic to these cells (Fig. 6*C*). Indeed, increased expression of QDPR by induction with tetracycline was lethal to cells (data not shown).

Having successfully created the [oe]WT line, further rounds of transfection were done to delete PTR1. The deletion of one copy of PTR1 ([oe]SKO) did not result in any changes in growth (doubling time 8.8 h) compared with the [oe]WT cells (Fig. 6*C*).
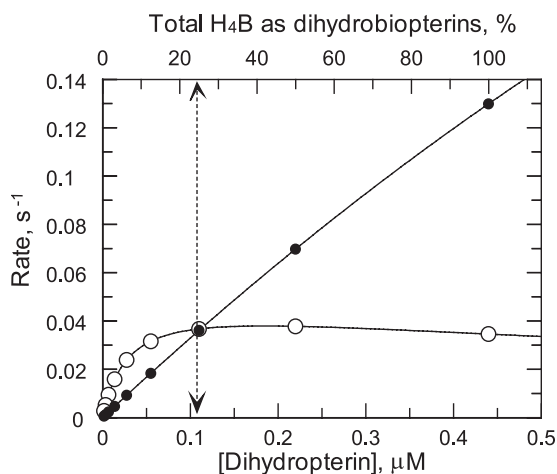

FIGURE 7. **Predicted kinetic behavior of PTR1 within intact *T. brucei*.** Data are fitted to the equation for high substrate inhibition over the possible ranges of H_2B (○) or qH_2B (●) that could occur should intracellular H_4B be converted to either of these substrates. The upper *x* axis shows the percentage conversion and the *vertical dotted line* indicates the concentration of either substrate that gives the same PTR1 activity.

However, the deletion of the second copy ([oe]DKO) resulted in a ~1.7-fold decrease in growth rate (generation time 15.3 h; Fig. 6*C*). The loss of both PTR1 genes and their expression were confirmed by Southern blot analysis and RT-PCR respectively (Fig. 6, *A* and *B*). [oe]DKO parasites were only viable in folate-rich medium supplemented with H_4B. While they continued to grow normally for 11 days in the absence of H_4B, cell numbers dropped precipitously thereafter, such that no surviving cells were evident by day 16 (Fig. 6*C*).

Experiments were then carried out to determine whether biopterin or H_2B could substitute for H_4B in supporting growth of [oe]DKO cells in low folate medium (Fig. 6*D*). In the absence of added pterin, the cells were completely dead by day 4, whereas addition of biopterin or H_2B prolonged survival to 14 and 16 days, respectively. Only when medium was supplemented with H_4B at each subculture were the trypanosomes able to grow normally. These results confirm the dual role of *Tb*PTR1 in the salvage and regeneration of H_4B, cementing its status as a validated drug target for the treatment of HAT.

DISCUSSION

The studies reported here have identified some striking differences in pterin metabolism between *T. brucei* and *L. major*. Our findings argue strongly in favor of the absence of a *bona fide* NADH-dependent QDPR in *T. brucei* for the following reasons. First, unlike *L. major* cell extracts, oxidation of NADH by $qDMH_2P$ catalyzed by procyclic-form lysates is non-linear and does not go to completion by recycling between the quinonoid and tetrahydro-forms. Second, NADH oxidation is not observed with the physiological substrate, qH_2B. Third, only cells overexpressing *Lm*QDPR display readily detectable QDPR activity with NADH as electron donor, indicating that the fail-
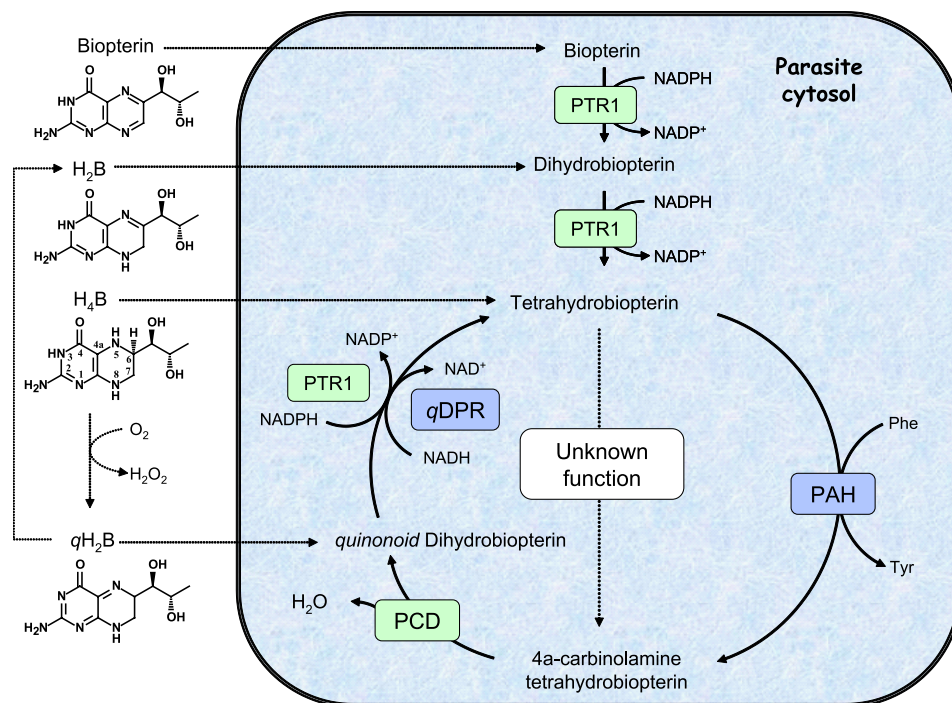

FIGURE 8. **Enzymes and metabolic pathways in *T. brucei* and *L. major*.** Enzymes present in both parasites are shown in *green* and enzymes only present in *L. major* are shown in *blue*. The *dotted lines* indicate pterins that can be taken up from the medium. An unknown hydroxylation reaction generating 4a-cabinolamine tetrahydrobiopterin is postulated to account for the essentiality of PTR1 in *T. brucei* and the ability of *Lm*QDPR to rescue *ptr1*^{−/−} mutants.

ure to detect activity in wild-type cell extracts was not due to artifacts such as endogenous inhibitors. Finally, these observations are entirely consistent with the absence of a credible QDPR orthologue in the *T. brucei* genome.

The exact nature of the reaction observed in procyclic-form *T. brucei* remains to be elucidated. At present we have established that all components of the assay are required, including HRP and H_2O_2, suggesting that the reaction has a requirement for qDMH$_2$P. The activity is heat sensitive and the amount of NADH oxidized is proportional to the amount of extract, suggesting a heat labile protein or metabolite may be involved. It also appears to be specific to *T. brucei* procyclic-form, because the activity is absent in bloodstream forms.

One important point for consideration is whether the QDPR activity associated with PTR1 is physiologically relevant to *T. brucei*. Our studies indicate that the total biopterin concentration in bloodstream forms is 440 nM and PTR1 is 2.5 nM. However, only 2% (10 nM) is present as biopterin or more likely as H_2B, since this is the end product of oxidation of H_4B or qH_2B (15, 16). Thus, under physiological conditions the enzyme is operating below the K_m^{app} value (29 nM) for H_2B. This supports the hypothesis that enzymes evolve to function at substrate concentrations equivalent to the enzyme K_m for the substrate (49, 50). As discussed by Nare *et al.* (20), substrate inhibition of an enzyme is probably non-physiological and insignificant *in vivo* (49), primarily due to the high energetic cost required for maintaining high substrate concentrations (50). Clearly, the intracellular activity of PTR1 must be restricted to the physiological range of intracellular substrate (*i.e.* up to 440 nM). Based on the kinetic parameters determined for the pure recombinant enzyme at physiological pH and ionic strength, it is possible to predict the behavior of the system when H_4B is converted to either qH_2B or H_2B (it is not possible to determine the kinetic behavior for biopterin by either the current HPLC or spectrophotometric methods). The predicted rate behavior in the physiological substrate range for these dihydropterins is shown in Fig. 7. What is striking from this analysis is that, with qH_2B as substrate, where $[S] \ll K_m$ ($K_m^{app} = 3,400$ nM, Table 1) the rate is essentially first order over the entire range of possible substrate concentrations *in vivo*, whereas the enzymatic rate with H_2B as substrate plateaus at ~ 100 nM ($K_m^{app} = 29$ nM) due to the effects of inhibition by substrate ($K_i^s = 1.2$ μM). Enzymatic rates for both substrates are the same at $[S] = 100$ nM, where $\sim 25\%$ of the total biopterin is oxidized to either qH_2B or H_2B. Finally, it is evident from Fig. 7 that H_2B is the preferential substrate at low $[S]$, whereas qH_2B is the preferential substrate at high $[S]$. Thus, despite the markedly different kinetic parameters for PTR1 with these substrates *in vitro*, both can be predicted to behave as physiologically relevant substrates in the whole cell.

The presence or absence of a *bona fide* NADH-dependent QDPR in these trypanosomatids has important implications for drug development against these diseases (Fig. 8). Both organisms possess PTR1 and PCD, whereas *T. brucei* lacks QDPR and PAH. The presence of PCD would suggest that 4a-carbinolamine tetrahydrobiopterin is being formed in these organisms. Certainly this would appear to be the case for *L. major* because

conversion of phenylalanine to tyrosine by PAH would involve conversion of H_4B to this intermediate. However, as mentioned in the introduction, this gene is not essential for *L. major* (26). We therefore propose that additional unknown hydroxylation reactions exist in these organisms that would account for the essential requirement for pterins. This would explain why PTR1 is essential in *T. brucei* and why $ptr1^{-/-}$ organisms can only be rescued with *Lm*QDPR as an add-back in the presence of H_4B in the growth medium. Although PTR1 is not an attractive drug target *per se* in *L. major*, we suggest that QDPR may well be. Gene knock-out studies should be attempted to assess this prediction.

In conclusion, our studies have established that PTR1 is a potential drug target in the African trypanosome, but not in cutaneous leishmaniasis, caused by *L. major*. The kinetic parameters obtained under physiological conditions support the idea that PTR1 would operate in intact cells to regenerate H_4B from either H_2B or qH_2B. The origin of these metabolites is currently under study in our laboratory.

REFERENCES

1. Kaufman, S. (1961) *J. Biol. Chem.* **236,** 804–810
2. Nagatsu, T., Levitt, M., and Udenfriend, S. (1964) *J. Biol. Chem.* **239,** 2910–2917
3. Lovenberg, W., Jequier, E., and Sjoerdsma, A. (1967) *Science.* **155,** 217–219
4. Tietz, A., Lindberg, M., and Kennedy, E. P. (1964) *J. Biol. Chem.* **239,** 4081–4090
5. Kaufman, S., Pollock, R. J., Summer, G. K., Das, A. K., and Hajra, A. K. (1990) *Biochim. Biophys. Acta.* **1040,** 19–27
6. Kwon, N. S., Nathan, C. F., and Stuehr, D. J. (1989) *J. Biol. Chem.* **264,** 20496–20501
7. Tayeh, M. A., and Marletta, M. A. (1989) *J. Biol. Chem.* **264,** 19654–19658
8. Mayer, B., and Hemmens, B. (1997) *Trends Biochem. Sci.* **22,** 477–481
9. Shiota, T., Disraely, M. N., and McCann, M. P. (1964) *J. Biol. Chem.* **239,** 2259–2266
10. Curtius, H. C., Heintel, D., Ghisla, S., Kuster, T., Leimbacher, W., and Niederwieser, A. (1985) *Eur. J. Biochem.* **148,** 413–419
11. Werner, E. R., Werner-Felmayer, G., Fuchs, D., Hausen, A., Reibnegger, G., Yim, J. J., Pfleiderer, W., and Wachter, H. (1990) *J. Biol. Chem.* **265,** 3189–3192
12. Huang, C. Y., and Kaufman, S. (1973) *J. Biol. Chem.* **248,** 4242–4251
13. Lazarus, R. A., Dietrich, R. F., Wallick, D. E., and Benkovic, S. J. (1981) *Biochemistry* **20,** 6834–6841
14. Kaufman, S. (1967) *J. Biol. Chem.* **242,** 3934–3953
15. Kirsch, M., Korth, H. G., Stenert, V., Sustmann, R., and De Groot, H. (2003) *J. Biol. Chem.* **278,** 24481–24490
16. Davis, M. D., Kaufman, S., and Milstien, S. (1988) *Eur. J. Biochem.* **173,** 345–351
17. Thöny, B., Auerbach, G., and Blau, N. (2000) *Biochem. J.* **347,** 1–16
18. Crabtree, M. J., Tatham, A. L., Hale, A. B., Alp, N. J., and Channon, K. M. (2009) *J. Biol. Chem.* **284,** 28128–28136
19. Beck, J. T., and Ullman, B. (1990) *Mol. Biochem. Parasitol.* **43,** 221–230
20. Nare, B., Hardy, L. W., and Beverley, S. M. (1997) *J. Biol. Chem.* **272,** 13883–13891
21. Kidder, G. W., and Dutta, B. N. (1958) *J. Gen. Microbiol.* **18,** 621–638
22. Kündig, C., Haimeur, A., Légaré, D., Papadopoulou, B., and Ouellette, M. (1999) *EMBO J.* **18,** 2342–2351
23. Bello, A. R., Nare, B., Freedman, D., Hardy, L., and Beverley, S. M. (1994)

Proc. Natl. Acad. Sci. U.S.A. **91,** 11442–11446

24. Cunningham, M. L., Titus, R. G., Turco, S. J., and Beverley, S. M. (2001) *Science* **292,** 285–287
25. Ma, D., Beverley, S. M., and Turco, S. J. (1996) *Biochem. Biophys. Res. Commun.* **227,** 885–889
26. Lye, L. F., Kang, S. O., Nosanchuk, J. D., Casadevall, A., and Beverley, S. M. (2011) *Mol. Biochem. Parasitol.* **175,** 58–67
27. Lye, L. F., Cunningham, M. L., and Beverley, S. M. (2002) *J. Biol. Chem.* **277,** 38245–38253
28. Moreira, W., Leblanc, E., and Ouellette, M. (2009) *Free Radic. Biol. Med.* **46,** 367–375
29. Nare, B., Garraway, L. A., Vickers, T. J., and Beverley, S. M. (2009) *Curr. Genet.* **55,** 287–299
30. Sienkiewicz, N., Ong, H. B., and Fairlamb, A. H. (2010) *Mol. Microbiol.* **77,** 658–671
31. Wirtz, E., Leal, S., Ochatt, C., and Cross, G. A. M. (1999) *Mol. Biochem. Parasitol.* **99,** 89–101
32. Brun, R., and Schönenberger, M. (1979) *Acta Trop.* **36,** 289–292
33. Greig, N., Wyllie, S., Patterson, S., and Fairlamb, A. H. (2009) *FEBS J.* **276,** 376–386
34. Sienkiewicz, N., Jaroslawski, S., Wyllie, S., and Fairlamb, A. H. (2008) *Mol. Microbiol.* **69,** 520–533
35. Lanham, S. M. (1968) *Nature* **218,** 1273–1274
36. Fukushima, T., and Nixon, J. C. (1980) *Anal. Biochem.* **102,** 176–188
37. Shanks, E. J., Ong, H. B., Robinson, D. A., Thompson, S., Sienkiewicz, N., Fairlamb, A. H., and Frearson, J. A. (2010) *Anal. Biochem.* **396,** 194–203
38. Pfleiderer, W. (1985) in *Chemistry and Biochemistry of Pterins* (Blakley, R. L., and Benkovic, S. J., eds) pp. 43–114, John Wiley & Sons, New York
39. Dawson, A., Gibellini, F., Sienkiewicz, N., Tulloch, L. B., Fyfe, P. K., McLuskey, K., Fairlamb, A. H., and Hunter, W. N. (2006) *Mol. Microbiol.* **61,** 1457–1468
40. Gourley, D. G., Luba, J., Hardy, L. W., Beverley, S. M., and Hunter, W. N. (1999) *Acta Crystallogr. D* **55,** 1608–1610
41. Jockers-Scherübl, M. C., Schirmer, R. H., and Krauth-Siegel, R. L. (1989) *Eur. J. Biochem.* **180,** 267–272
42. Opperdoes, F. R., Baudhuin, P., Coppens, I., De Roe, C., Edwards, S. W., Weijers, P. J., and Misset, O. (1984) *J. Cell Biol.* **98,** 1178–1184
43. Keita, M., Vincendeau, P., Buguet, A., Cespuglio, R., Vallat, J. M., Dumas, M., and Bouteille, B. (2000) *Exp. Parasitol.* **95,** 19–27
44. Murr, C., Widner, B., Wirleitner, B., and Fuchs, D. (2002) *Curr. Drug. Metab.* **3,** 175–187
45. Yoshida, S., Lee, Y. H., Hassan, M., Shoji, T., Onuma, K., Hasegawa, H., Nakagawa, H., Serizawa, S., and Amayasu, H. (2001) *Respiration* **68,** 299–306
46. Scott, D. A., Moreno, S. N., and Docampo, R. (1995) *Biochem. J.* **310,** 789–794
47. Hasegawa, H., Nakanishi, N., and Akino, M. (1978) *J. Biochem.* **84,** 499–506
48. Wang, J., Leblanc, E., Chang, C. F., Papadopoulou, B., Bray, T., Whiteley, J. M., Lin, S. X., and Ouellette, M. (1997) *Arch. Biochem. Biophys.* **342,** 197–202
49. Fersht, A. R. (1974) *Proc. R. Soc. Lond B Biol. Sci.* **187,** 397–407
50. Copeland, R. A. (2005) *Evaluation of Enzyme Inhibitors in Drug Discovery: A Guide for Medicinal Chemists and Pharmacologists* p. 77, John Wiley & Sons, Hoboken
51. Vickers, T. J., Orsomando, G., de la Garza, R. D., Scott, D. A., Kang, S. O., Hanson, A. D., and Beverley, S. M. (2006) *J. Biol. Chem.* **281,** 38150–38158